Evidence of Cosmic-Ray Excess from Local Giant Molecular Clouds

Vardan Baghmanyan

Institute of Nuclear Physics PAN, Krakow, Poland

Seminar at the IFJ PAN, 18 May 2021

About the project

The Astrophysical Journal Letters, 901:L4 (6pp), 2020 September 20 https://doi.org/10.3847/2041-8213/abb5f8

Evidence of Cosmic-Ray Excess from Local Giant Molecular Clouds

Vardan Baghmanyan[1,4], Giada Peron[2], Sabrina Casanova[1,2], Felix Aharonian[2,3,4], and Roberta Zanin[5]
[1] Institute of Nuclear Physics PAN, Radzikowskiego 152, 31-342 Kraków, Poland; vardan.baghmanyan@ifj.edu.pl
[2] Max-Planck-Institut für Kernphysik, P.O. Box 103980, D-69029 Heidelberg, Germany
[3] Dublin Institute for Advanced Studies, 31 Fitzwilliam Place, Dublin 2, Ireland
[4] High Energy Astrophysics Laboratory, RAU, 123 Hovsep Emin Street, Yerevan 0051, Armenia
[5] CTA observatory, Via Piero Gobetti 93/3, I-40129 Bologna, Italy
Received 2020 June 7; revised 2020 August 14; accepted 2020 September 6; published 2020 September 18

Abstract

We report the analysis of the Fermi-Large Area Telescope data from six nearby giant molecular clouds (MCs) belonging to the Gould Belt and the Aquila Rift regions. The high statistical γ-ray spectra above 3 GeV well described by power laws make it possible to derive precise estimates of the cosmic-ray (CR) distribution in the MCs. The comparison of γ-ray spectra of Taurus, Orion A, and Orion B clouds with the model expected from Alpha Magnetic Spectrometer (AMS-02) CR measurements confirms these clouds as passive clouds, immersed in an AMS-02-like CR spectrum. A similar comparison of Aquila Rift, Rho Oph, and Cepheus spectra yields significant deviation in both spectral indices and absolute fluxes, which can imply an additional acceleration of CRs throughout the entire clouds. Besides, the theoretical modeling of the excess γ-ray spectrum of these clouds, assuming π^0-decay interaction of CRs in the cloud, gives a considerable amount of an enhanced CR energy density and it shows a significant deviation in spectral shapes compared to the average AMS-02 CR spectrum between 30 GeV and 10 TeV. We suggest that this variation in the CR spectrum of Cepheus could be accounted for by an efficient acceleration in the shocks of winds of OB associations, while in Rho Oph, similar acceleration can be provided by multiple T-Tauri stars populated in the whole cloud. In the case of Aquila Rift, the excess in absolute CR flux could be related to an additional acceleration of CRs by supernova remnants or propagation effects in the cloud.

https://iopscience.iop.org/article/10.3847/2041-8213/abb5f8

Outline

- Galactic cosmic-ray (CR) spectrum: direct and indirect studies
- The interstellar medium and molecular clouds
- Previous CR estimations through the MCs study with Fermi-LAT
- Selected MCs, analysis technique with Fermi-LAT and the results
- Theoretical interpretation
- Summary and future perspectives

Outline

- Galactic cosmic-ray (CR) spectrum: direct and indirect studies
- The interstellar medium and molecular clouds
- Previous CR estimations through the MCs study with Fermi-LAT
- Selected MCs, analysis technique with Fermi-LAT and the results
- Theoretical interpretation
- Summary and future perspectives

The high energy Galactic CR spectrum

What do we know about CRs?

- CRs consist mainly of primary protons, nuclei and electrons directly accelerated to relativistic energies by powerful objects, such as supernova remnants (SNRs).
- A change of the spectral index (E^−2.7 to E^−3.1) at an energy of about 10^15 eV is known as the CR knee.
- The flattening around 5 EeV called ankle.
- The average energy density of CRs in the Galactic Disk estimated by CR direct measurements is about Wcr ≈ 1 eV/cm3 (More than 90 percent of this density is contributed by particles with energy ≤ 100 GeV).
- The p/e at GeV energies is about 100 and >1000 at 1 TeV. It is usually assumed to be around 100 in the case of Galactic sources, while a value of 10 is typical for extragalactic sources.
- The pressure of CRs is comparable with the pressure of galactic magnetic fields, as well as with the turbulent and thermal pressure of the interstellar gas.

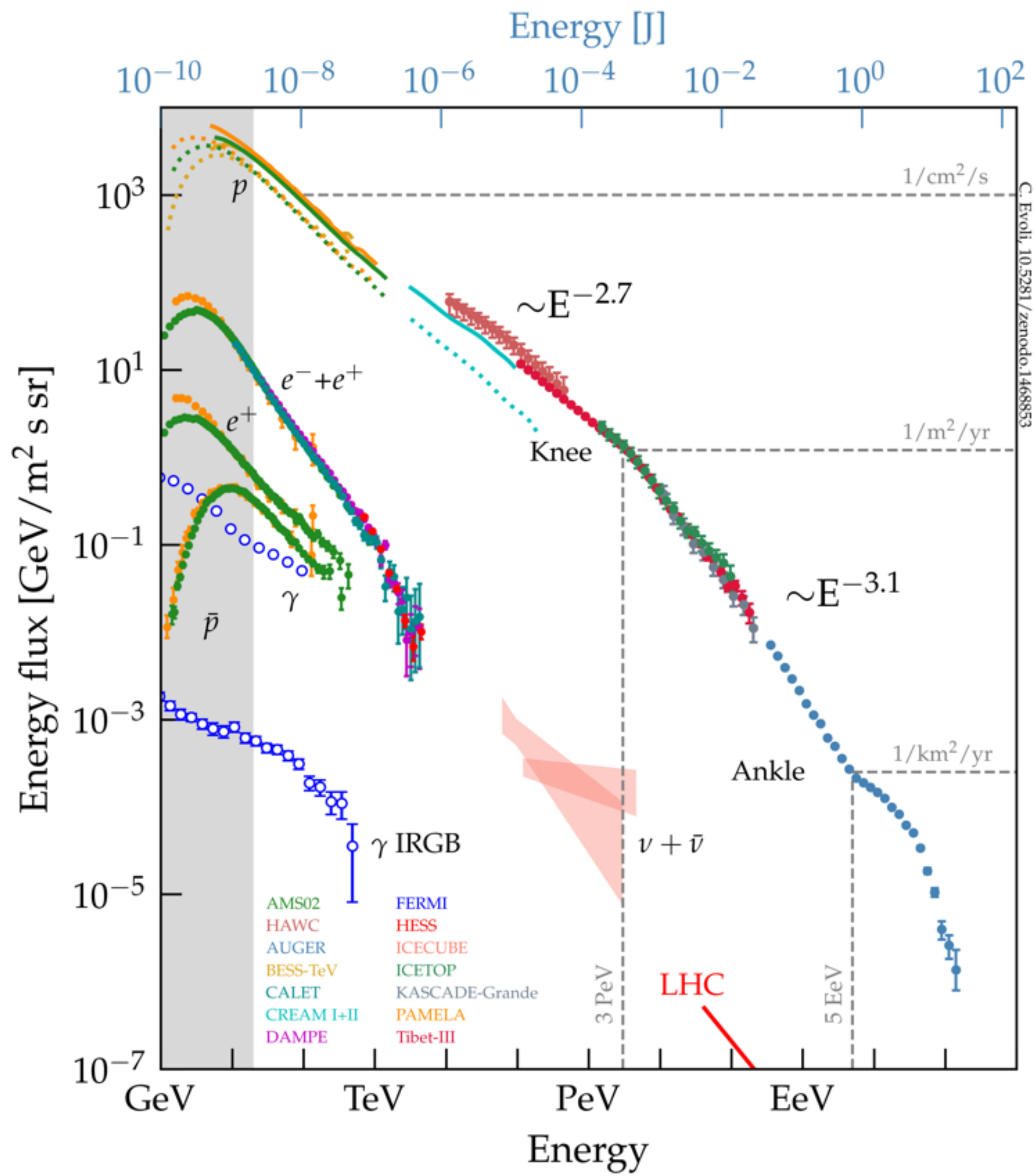

The high energy Galactic cosmic-ray spectrum

What do we don’t know about Galactic CRs?

- We do not know exactly what part of the observed CR spectrum has Galactic origin. Below the knee or beyond it?
- It is believed that SNRs are the major source population in our Galaxy responsible for the observed CRs.

Should we rule out other potential source populations like pulsars, **young stars with powerful mechanical winds**, microquasars, gamma-ray bursts, etc?

- We do not know what powers the CR accelerators, and how they work.

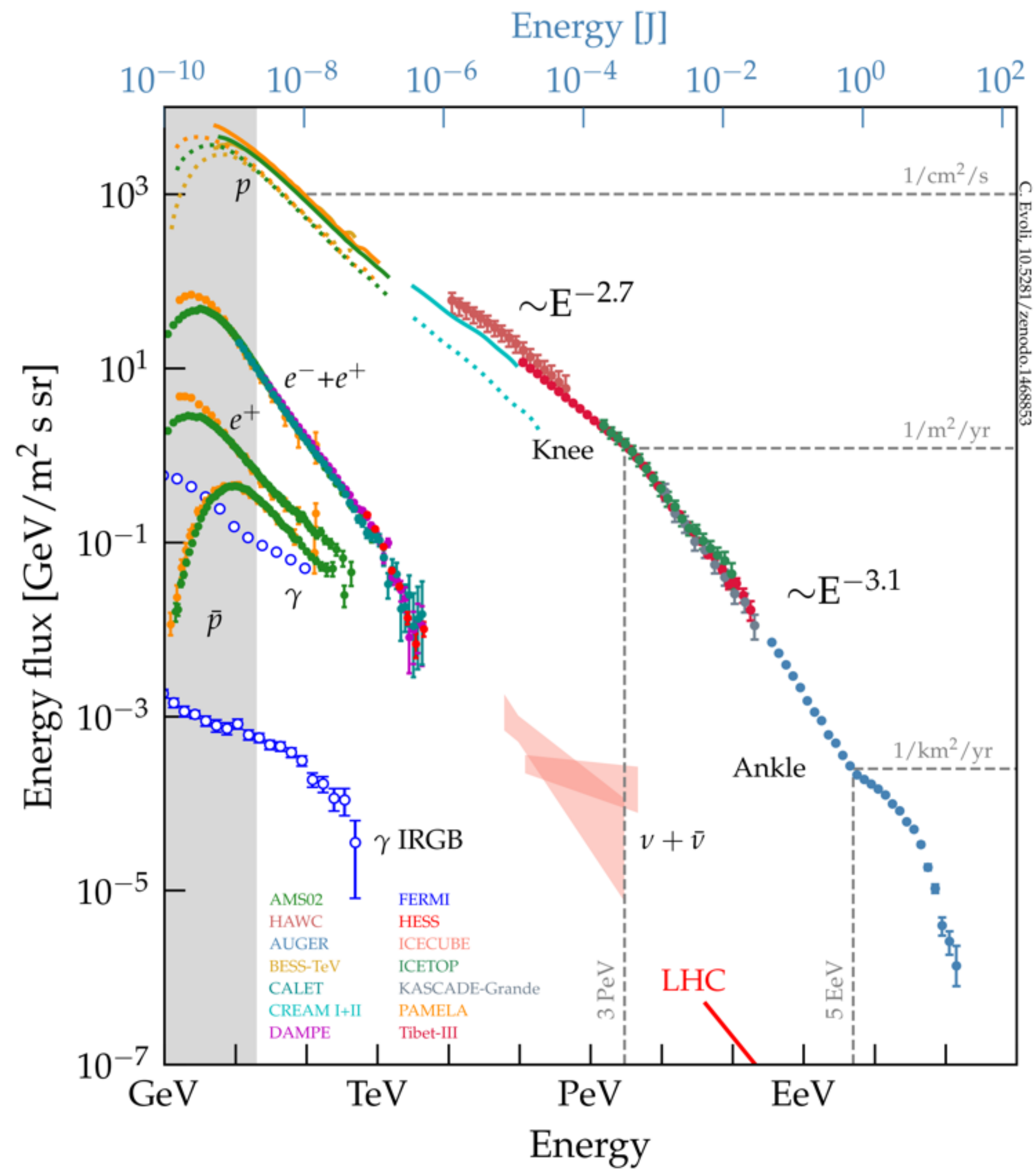

The high energy Galactic CR spectrum

What do we don't know about Galactic CRs?

- Still it is not clear the origin of discrepant hardening of the elemental spectra above ~200 GeV/nucleon as well as the spectral difference between the protons and helium nuclei measured by the CREAM experiment.

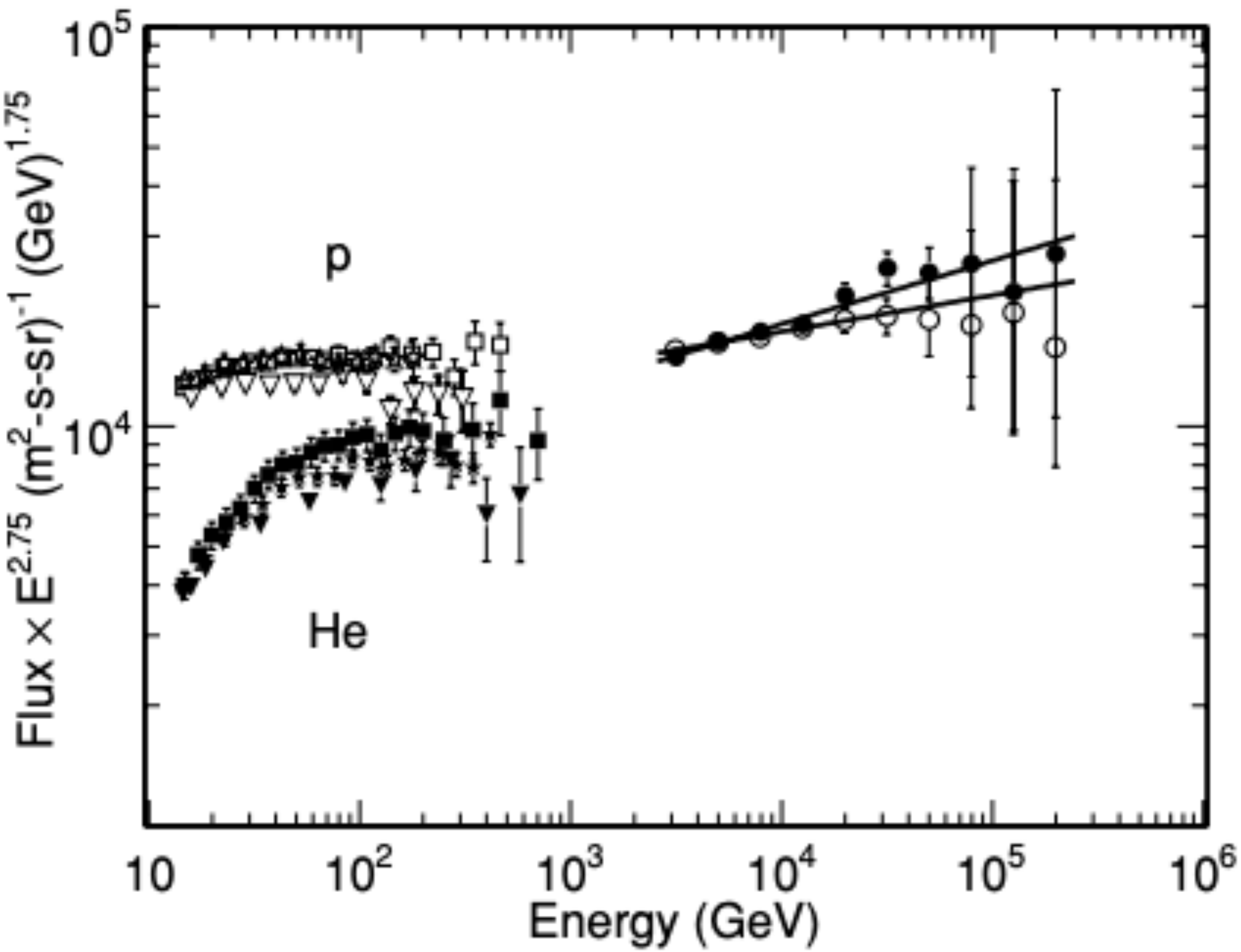

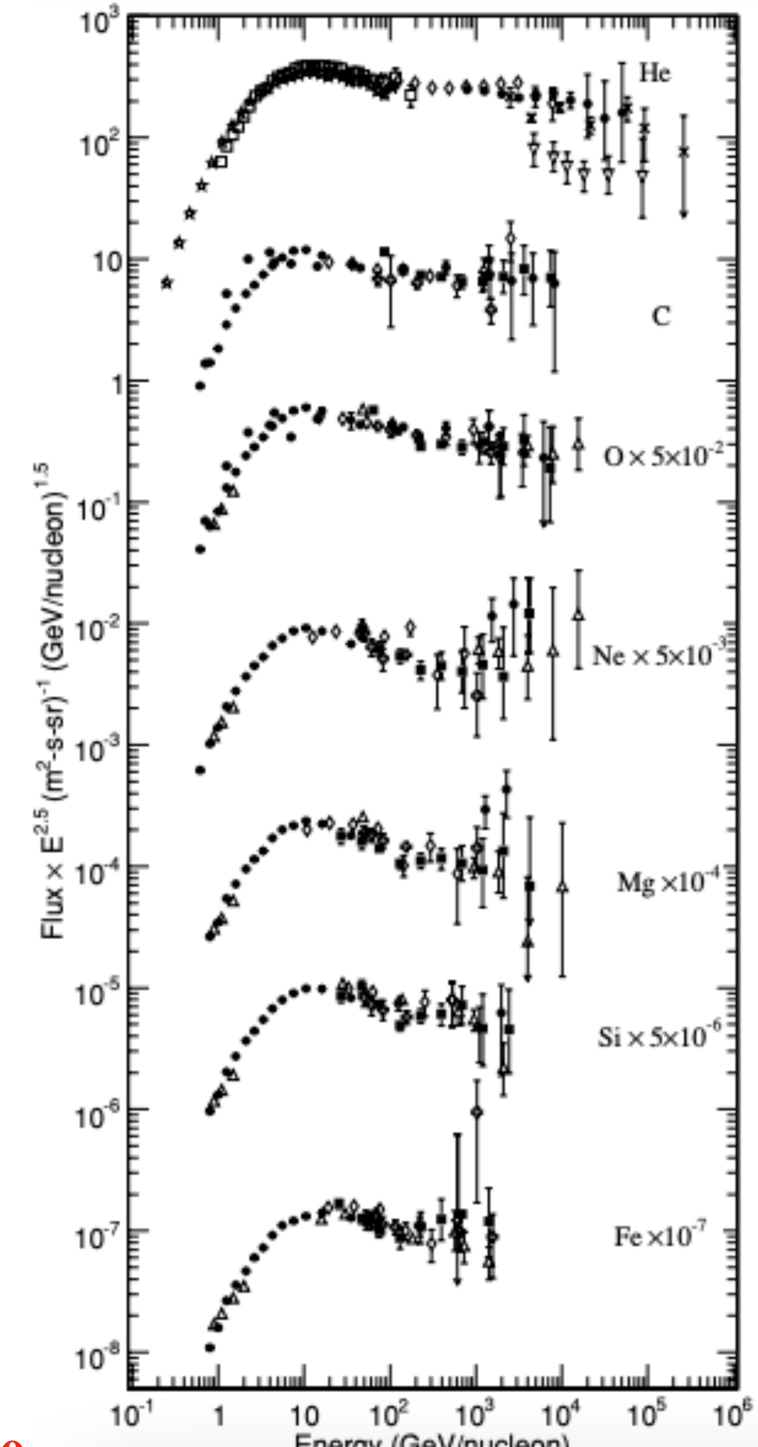

Ahn et al. 2010

Galactic CR studies through the diffuse γ-ray emission

- The EGRET data on the diffuse γ-ray emission from the Galactic plane at low latitudes ($-2 < b < 2$) showed evidence of a softer >4 GeV γ-ray spectrum in the outer Galaxy compared to the inner parts, which indicates a variation of CR spectrum with the Galactic radius (Hunter et al. 1997).
- HESS detected VHE diffuse γ-ray emission from the Galactic Center Ridge, which was explained by a significantly harder CR spectrum compared to local CR measurements (Aharonian et al. 2006).
- The measured gas emissivity spectra measured by indirect study with Fermi-LAT confirm that the CR proton density decreases with Galactocentric distance beyond 5 kpc from the Galactic Center. The measurements also show a softening of the proton spectrum with Galactocentric distance. (Acero et al. 2016).

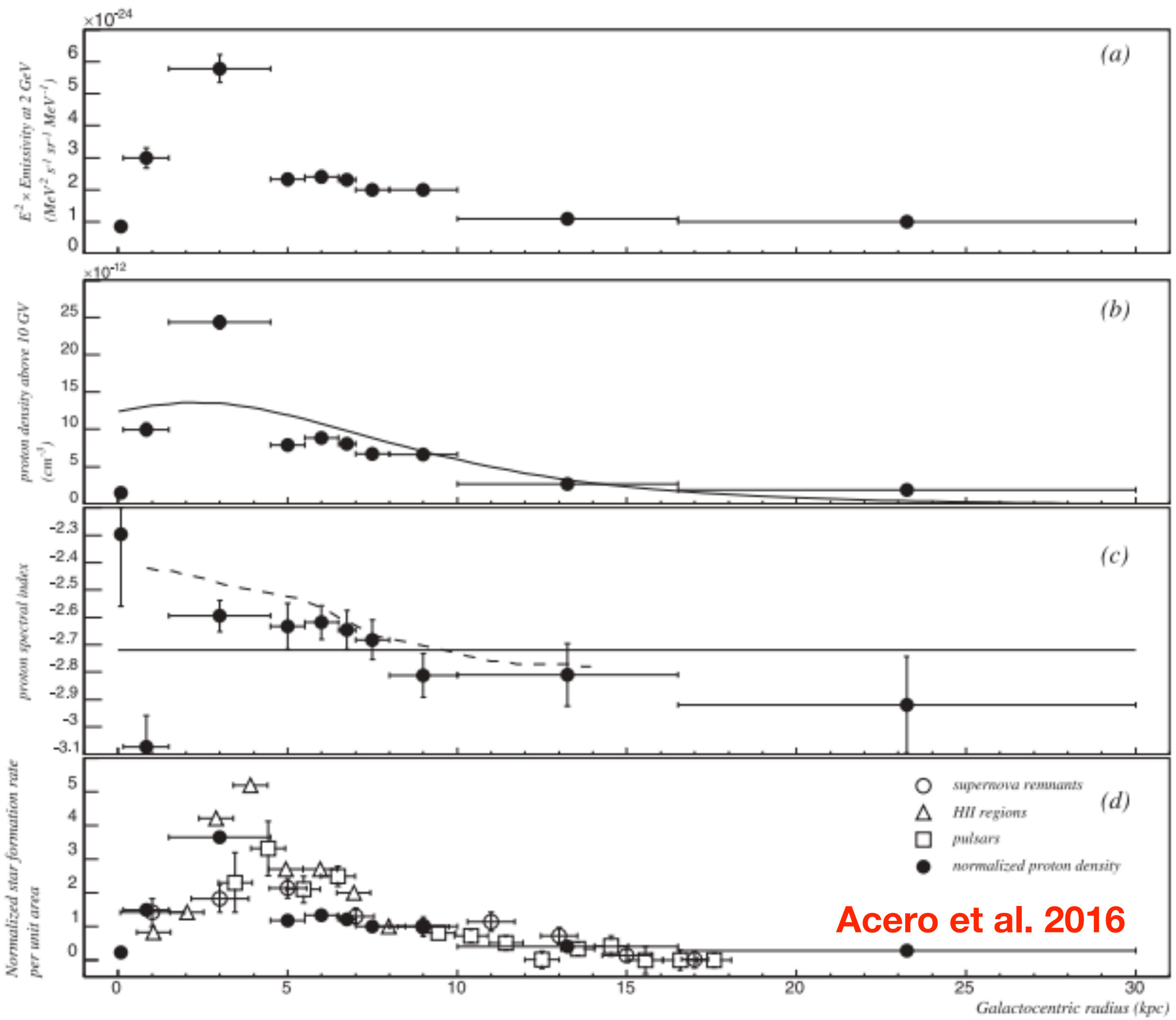

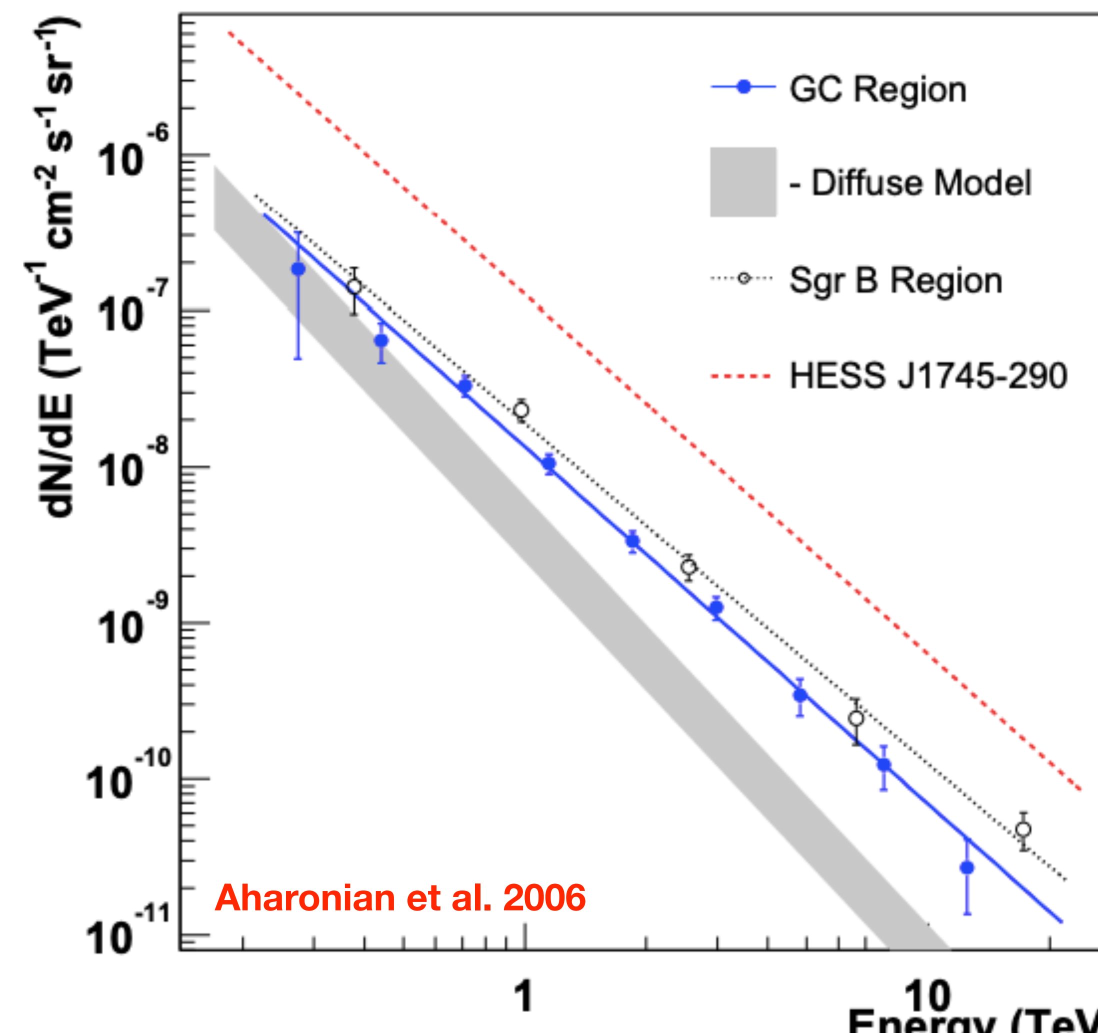

Outline

- Galactic cosmic-ray (CR) spectrum: direct and indirect studies
- The molecular clouds and star forming regions
- Previous CR estimations through the MCs study with Fermi-LAT
- Selected MCs, analysis technique with Fermi-LAT and the results
- Theoretical interpretation
- Summary and future perspectives

The Interstellar Medium (ISM)

Main Components of the ISM

- Hydrogen: neutral, ionized or molecular - 75%
- Helium and other molecules (CO, CN, …) - 24%
- Dust - 1%

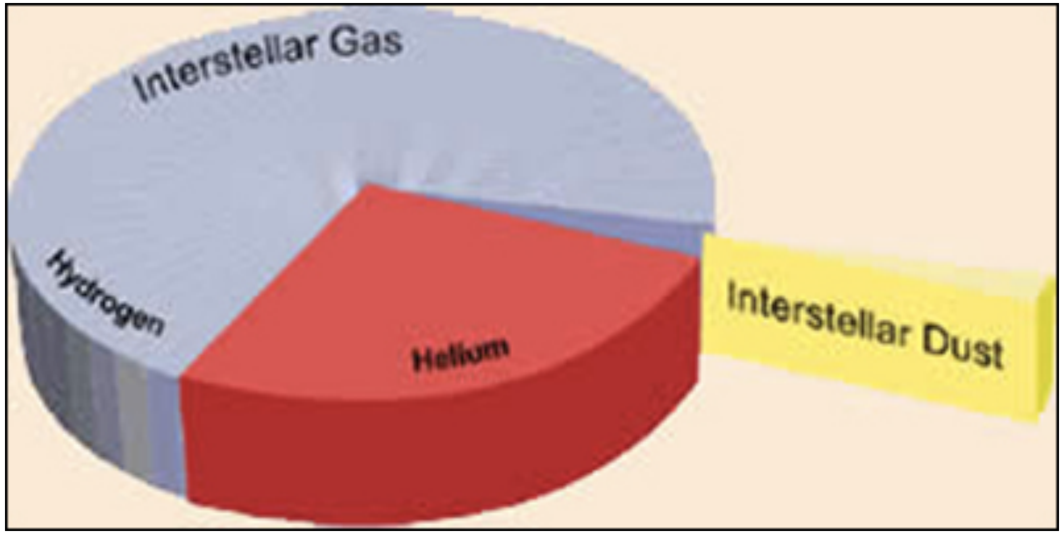

Locale	Density g/cm^3
Air in room	1.2×10^{-3}
Nebula around forming star	1×10^{-8}
Vacuum in lab	1×10^{-12}
Orion Nebula	1×10^{-21}
Typical Interstellar Space	1×10^{-24}

Hydrogen and dust in the Galaxy: molecular clouds

Hydrogen

Depends on the phase of the interstellar medium.

Phase 1: Cold (10's K)

Forms molecules, that results to formation of the dark nebula in the coldest regions, where the dense concentrations of gas and dust are called molecular clouds.

Phase 2: Warm (100 to 1000's K)

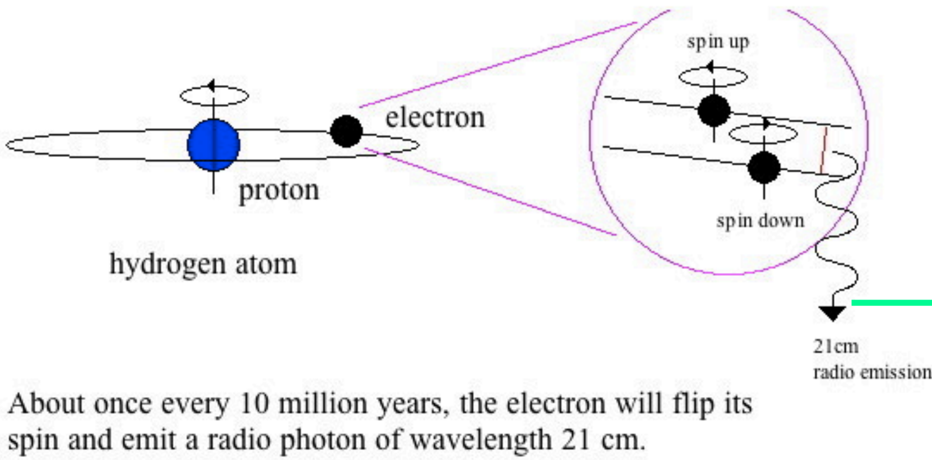

Phase 3: Hot (millions K)

Usually, occur when a cloud of neutral hydrogen is ionised by the UV radiation from young, massive stars.

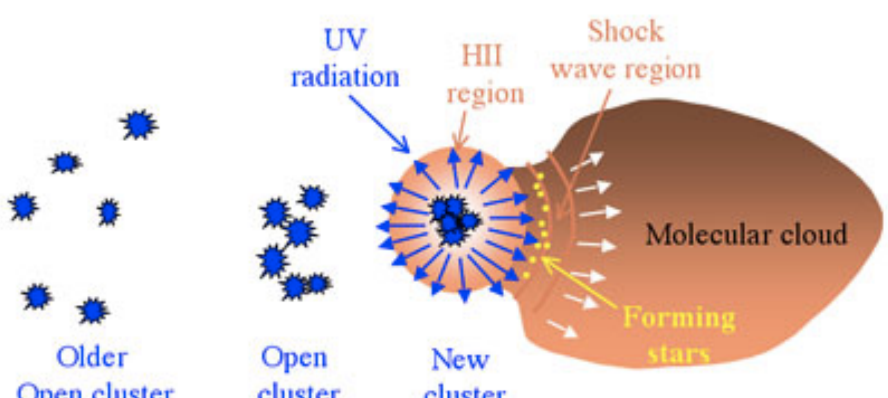

Dust

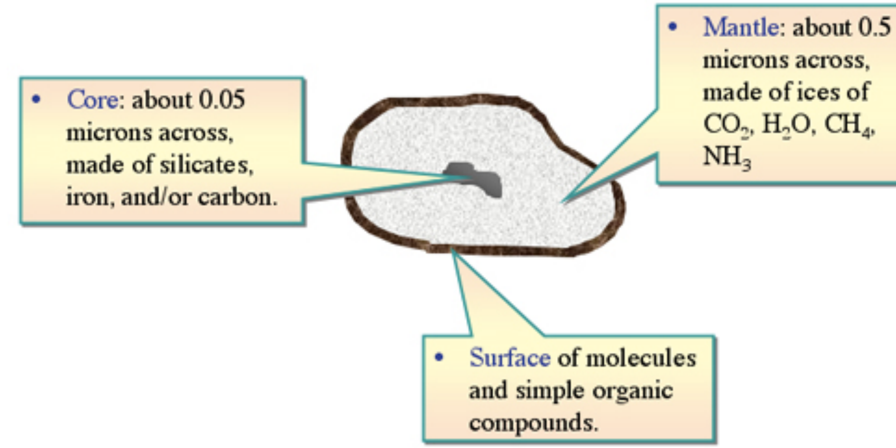

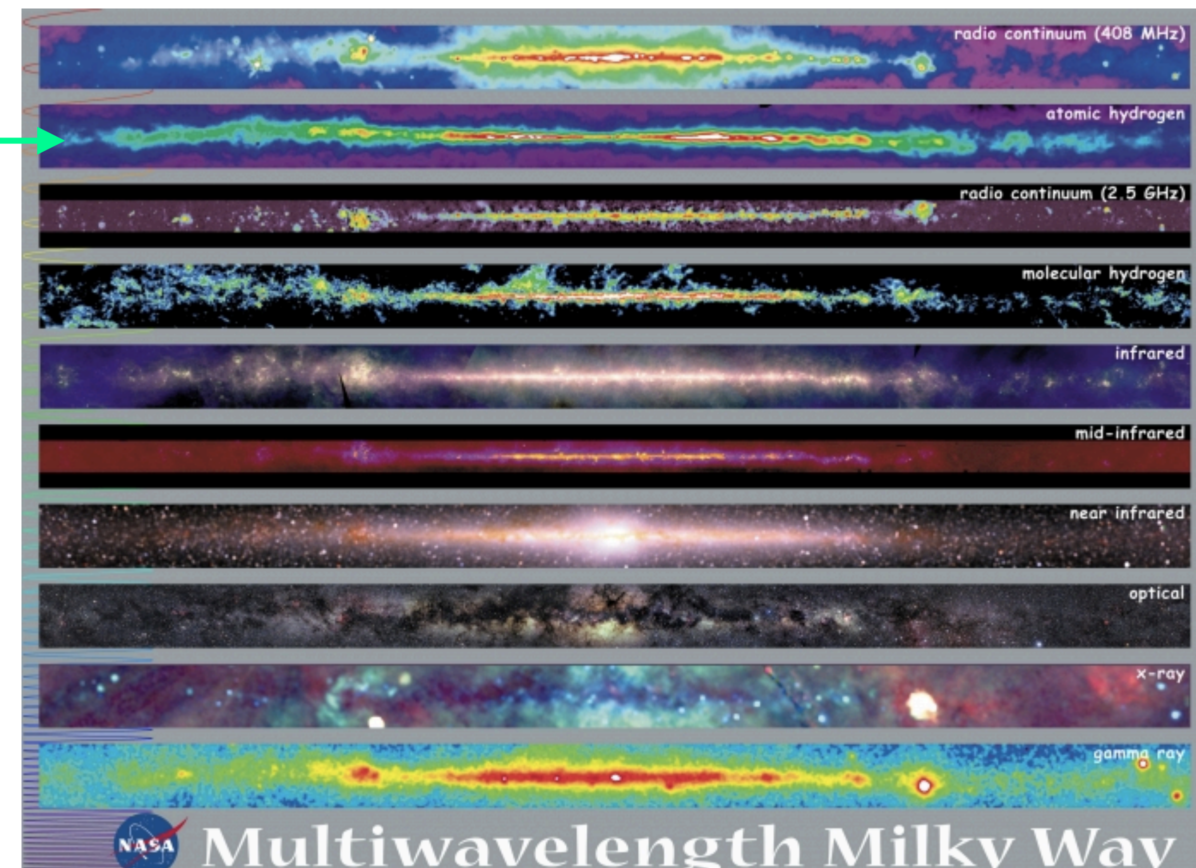

Microwave and thermal emission from molecular clouds

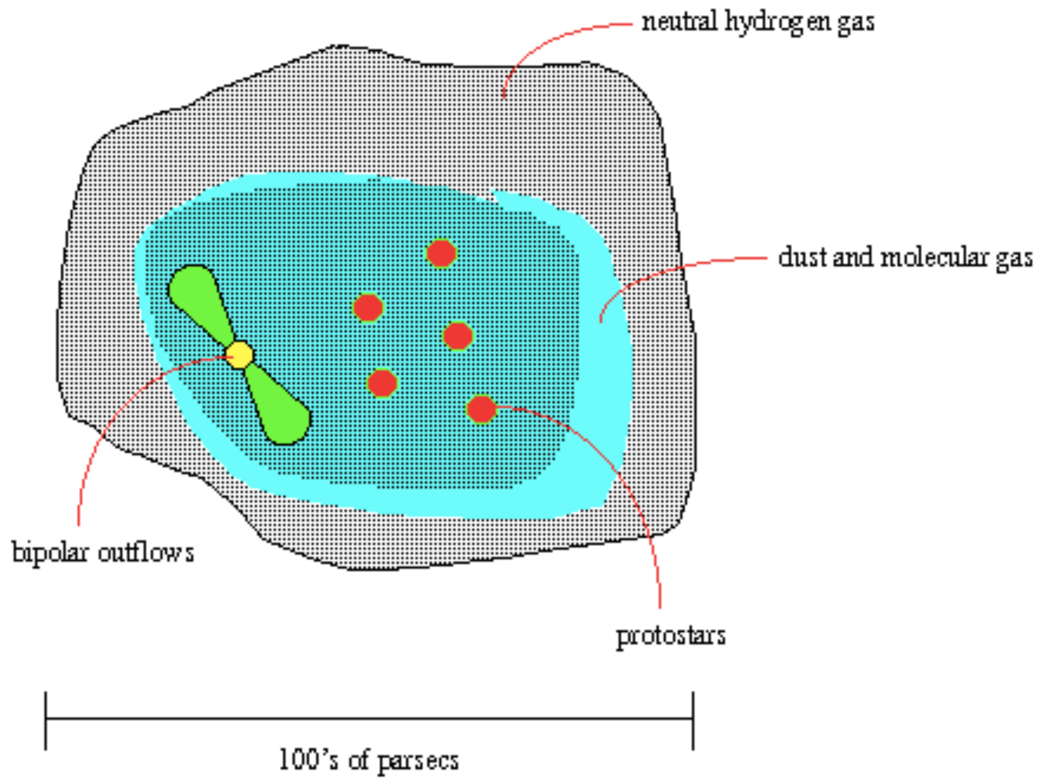

Low temperature (only a few 10's K) supports the formation of H2 and CO molecules on the surface of dust grains forming molecular clouds.

Dust

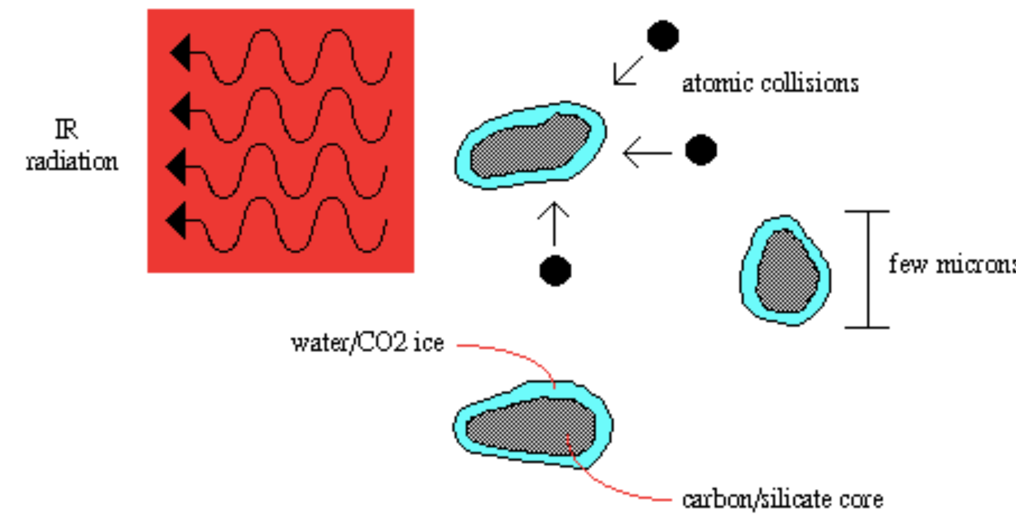

Carbon monoxide molecule (CO)

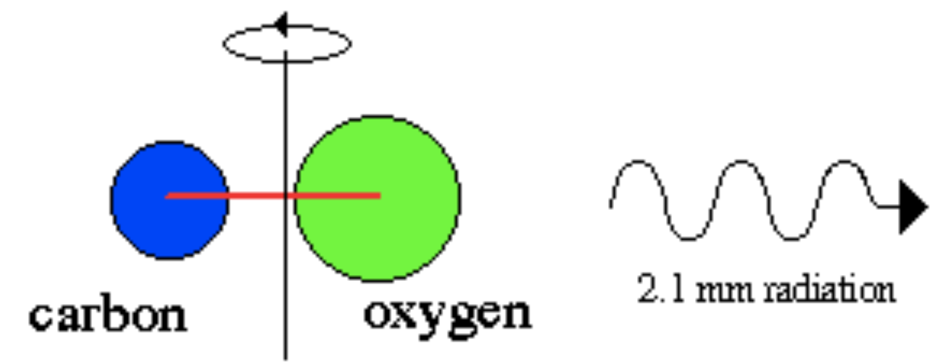

	Diffuse Atomic	Diffuse Molecular	Translucent	Dense Molecular
Defining Characteristic	$f^n_{H_2} < 0.1$	$f^n_{H_2} > 0.1$ $f^n_{C+} > 0.5$	$f^n_{C+} < 0.5$ $f^n_{CO} < 0.9$	$f^n_{CO} > 0.9$
A_V (min.)	0	~0.2	~1–2	~5–10
Typ. n_H (cm^{-3})	10–100	100–500	500–5000?	$>10^4$
Typ. T (K)	30–100	30–100	15–50?	10–50
Observational Techniques	UV/Vis H I 21-cm	UV/Vis IR abs mm abs	Vis (UV?) IR abs mm abs/em	IR abs mm em

The main tracers of molecular clouds for gamma-ray studies

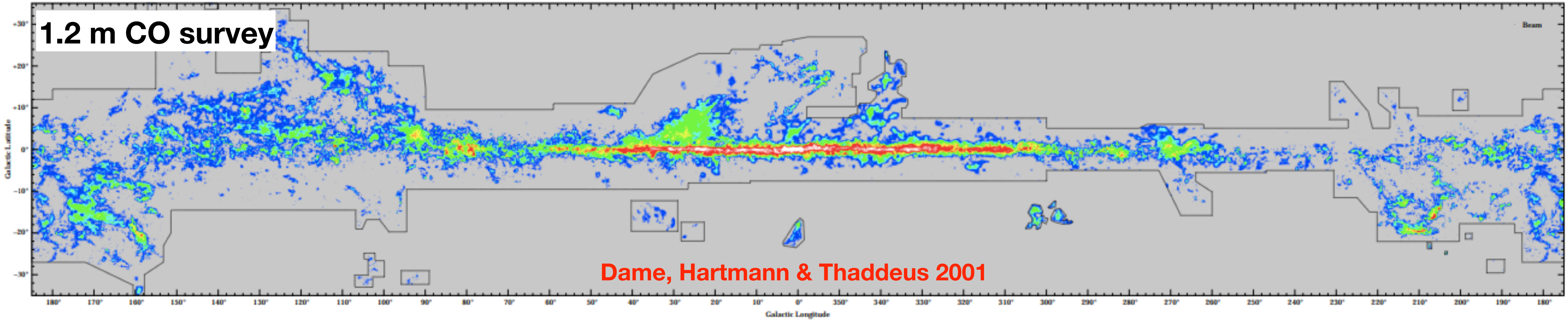

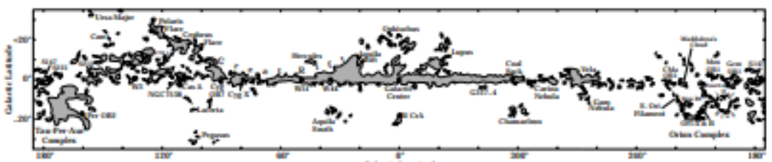

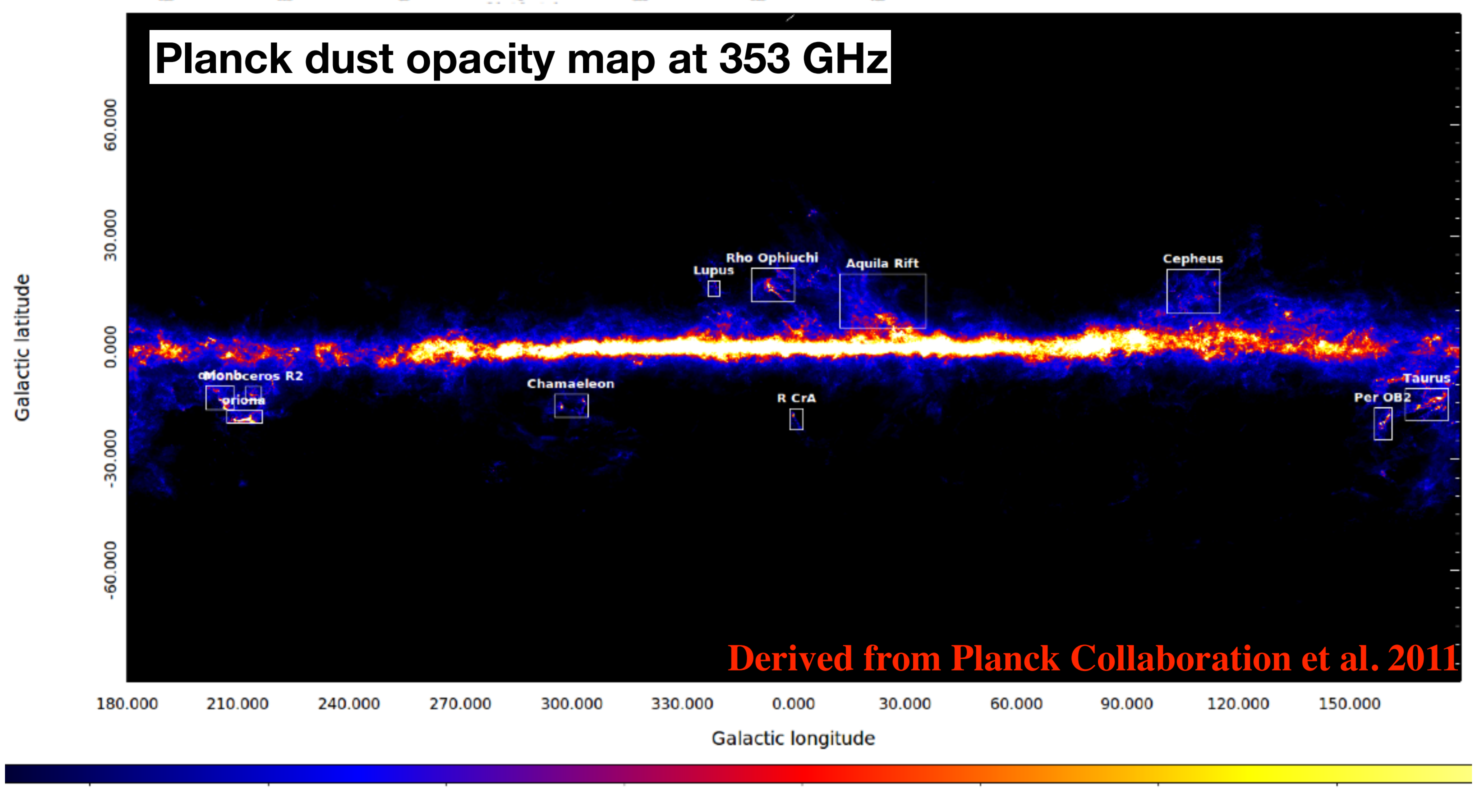

Dame et al. 1987

MOLECULAR GAS WITHIN 1 KILOPARSEC OF SUN

Region	l_{min}	l_{max}	b_{min}	b_{max}	v (km s^{-1})	D (pc)	Ref.	M ($10^5\ M_\odot$)	$\bar{z}$[a] (pc)	σ_z[b] (pc)
Aquila Rift	18°.5 34	34° 44	−6° −4	10° 4	8	200	1	1.5	9	15
Cloud A	44	49.5	−4	2	27	500	1	0.4[c]	−7	14
Cloud B	44	54	−4	5	7	300	1	0.4[c]	0	11
Cloud C	50	55	−1	3.5	24	500	1	0.3	5	12
Vul Rift	54	63	−3	5	10	400	1	0.8	5	12
Cyg Rift	63	86.5	−4	4	7	700	1	8.6[d]	−4	24
Cyg OB7	87	99	−3	8	−1	800	1	7.5	41	52
Lindblad Ring	100	164	−4	10	1	300	2	1.6	22	28
"−12 km/s"	102	161	−4	10	−12	800	3	8.7	44	59
Cepheus	100	120	11	22	−5	450	4	1.9	131	133
Taurus	163	178	−22	−9.5	5	140	5	0.3	−37	38
Per OB2	154 163	162.5 171	−25 −9	−7 −6	5 −3	350	5	1.3	−84	92
Mon OB1	197.5	205	−1	4	7	800	7	1.6	17	22
Orion A	208.5	218	−21	−14.5	5	500	6	1.6	−163	164
Orion B	202.5	208	−21	−6	5	500	6	1.7	−129	132
Mon R2	210	218	−14	−10	7	830	6	1.2	−182	183
Vela Sheet	272	279	−3	8	0	425	8	0.8	9	19
Cham	295	305	−20	−12	4	215	9	0.1	−60	60
Coalsack	300	307	−4	3	−4	175	10	0.04	−2	5
G317 − 4	315	320	−6	−2	−6	170	11	0.03	−11	11
Lupus	333	346	4	22	5	170	8	0.3	32	35
ρ Oph	350 356	2 5	13 3	24 12.5	3	165	12	0.3	35	39
R CrA	357	4	−22	−14	6	150	13	0.03	−55	55

Outline

- Galactic cosmic-ray (CR) spectrum: direct and indirect studies
- The interstellar medium and molecular clouds
- Previous CR estimations through the MCs study with Fermi-LAT
- Selected MCs, analysis technique with Fermi-LAT and the results
- Theoretical interpretation
- Summary and future perspectives

Previous CR estimations through the MCs study with Fermi-LAT

<u>**Neronov et al. 2012**</u> found that the GCR spectrum has a low-energy break with the spectral slope hardening by 1.1 +/- 0.3 at an energy of E = (9 +/- 3) GeV.

<u>**Ackermann et al. 2012**</u> found a variation of the CR density by ~20% in the neighbourhood of the solar system from 250 MeV to 10 GeV.

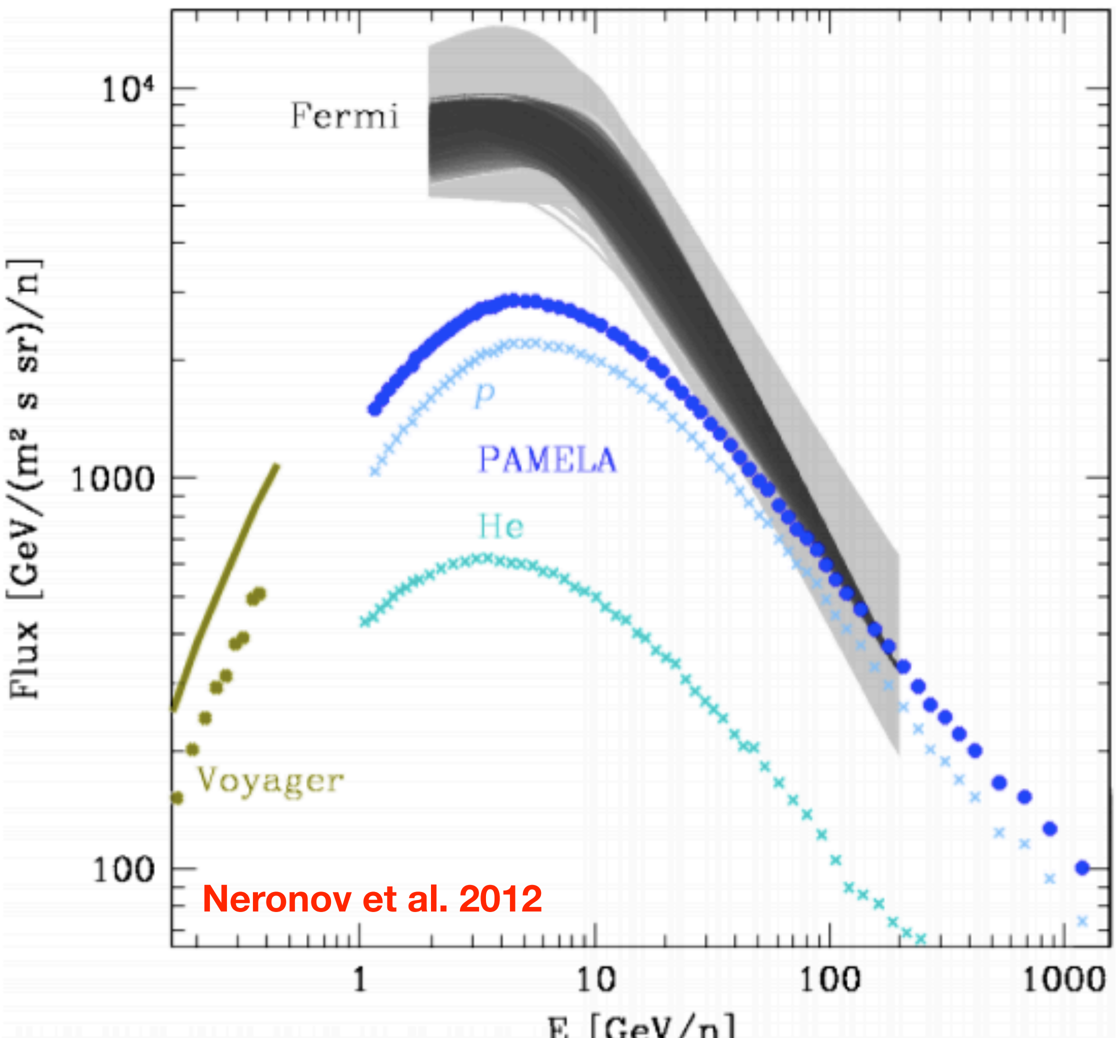

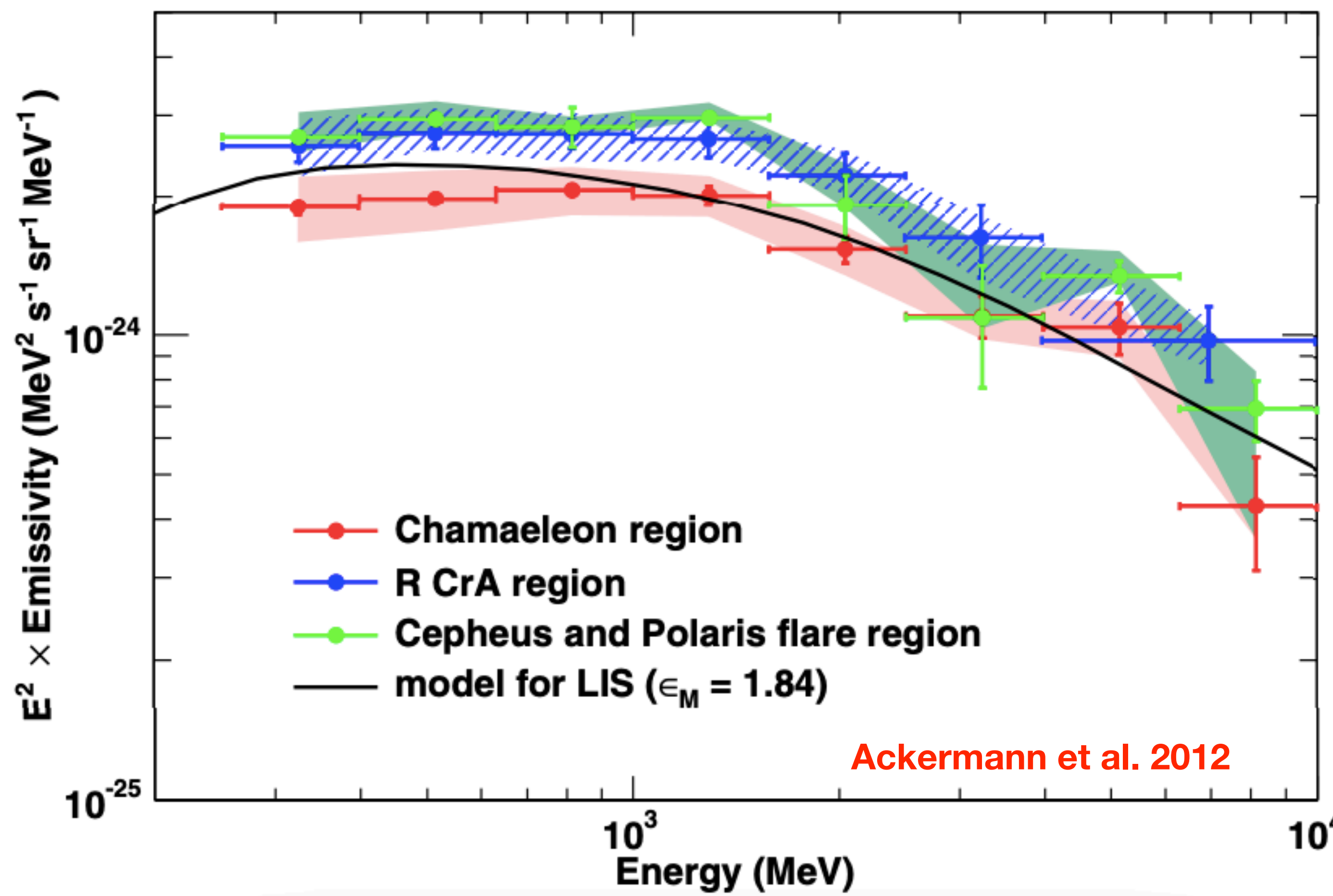

Previous CR estimations through the MCs study with Fermi-LAT

- The proton spectrum of Taurus, Persues OB2, and Mon R2 are described well by the locally measured proton spectrum by PAMELA.
- For Rho Oph, the derived CR spectrum is harder and total flux is lower than those observed by PAMELA (2.6 ± 0.3).
- The CR spectra of R CrA, Orion A, Orion B, and Chamaeleon show enhancement of CRs compared to the local CR flux at low energies. At high energies the spectrum shape is very similar to the one of the local CR.

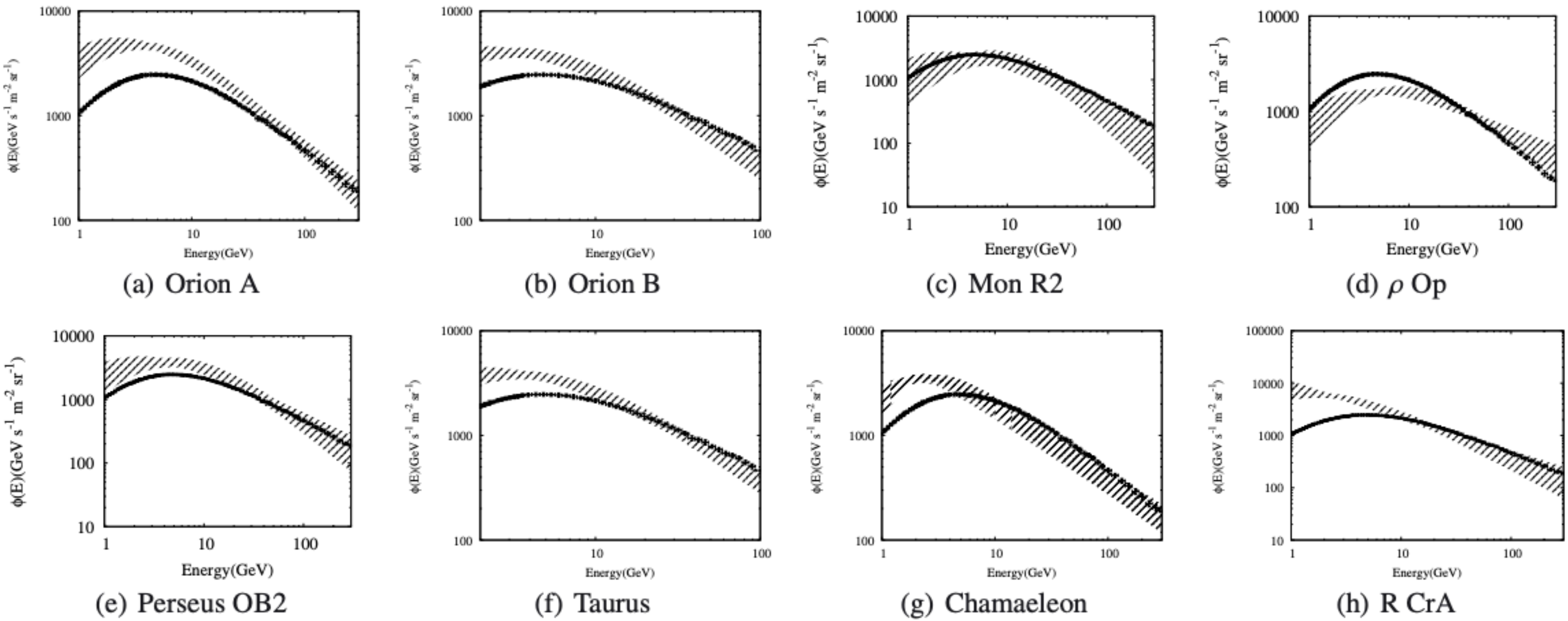

(a) Orion A (b) Orion B (c) Mon R2 (d) ρ Op (e) Perseus OB2 (f) Taurus (g) Chamaeleon (h) R CrA

Yang et al. 2014

The main tracers of molecular clouds

According to this study, several clouds in the galactocentric 4–6 kpc ring show evidence of enhanced CR density, which was interpreted by a possible contribution from active CR accelerators near MCs or an increase of CR density toward the GC.

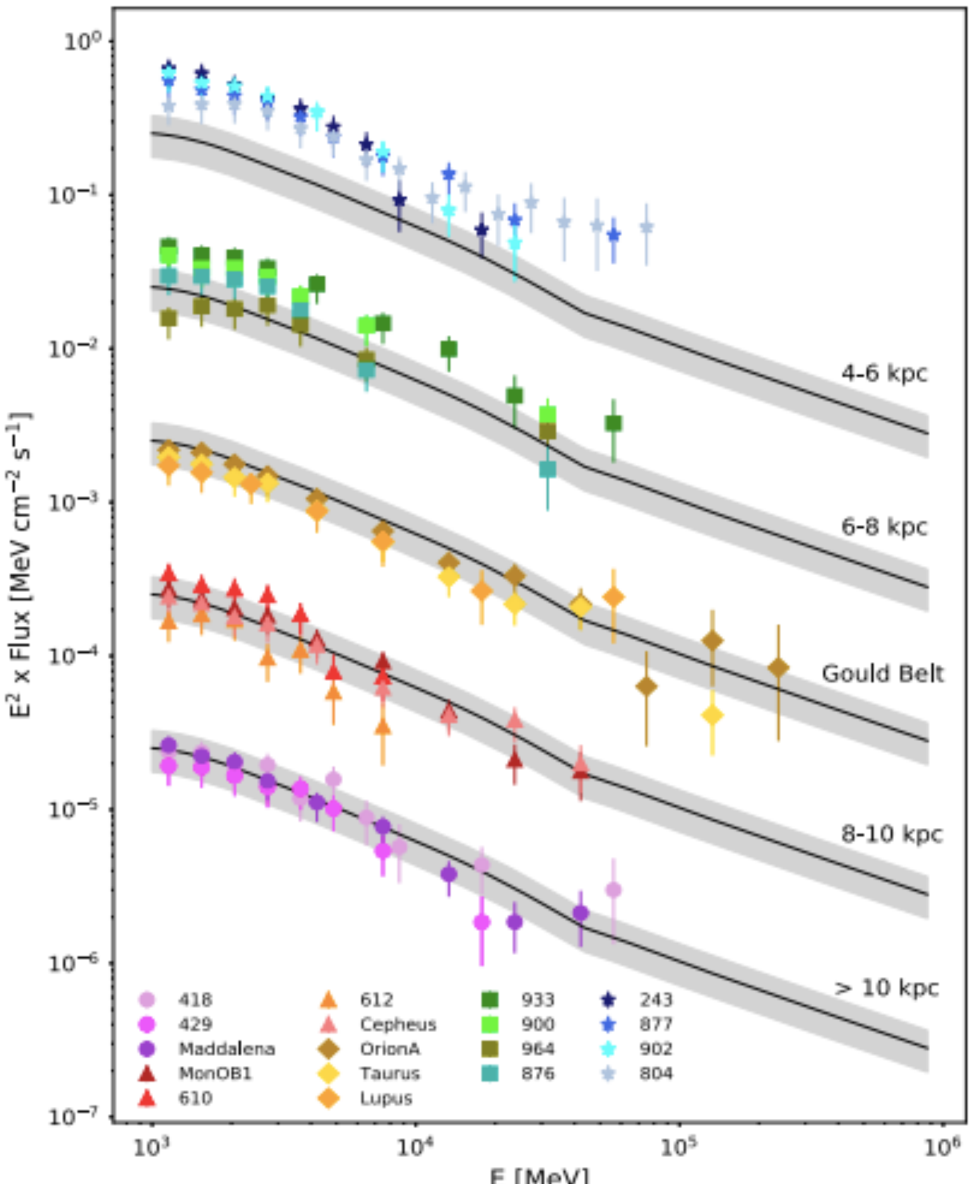

Cloud	l (deg)	b (deg)	Mass ($10^5 M_\odot$)	d (kpc)	R_{GC} (kpc)	A
243	42.04	−0.36	30 ± 10	7.9 ± 0.6	5.8	0.47
418	111.45	0.79	8 ± 3	4.1 ± 0.6	10.6	0.46
429	109.84	−0.29	10 ± 4	3.9 ± 0.6	10.3	0.67
610	142.40	1.38	0.3 ± 0.4	0.7 ± 0.5	8.9	0.61
612	126.87	−0.66	0.3 ± 0.5	0.6 ± 0.5	8.7	0.83
804	328.58	0.4	24 ± 8	5.7 ± 0.6	4.6	0.75
876	323.61	0.22	60 ± 18	10.2 ± 0.4	6.0	0.58
877	333.46	−0.31	13 ± 4	3.4 ± 0.4	5.5	1.11
900	318.07	−0.21	47 ± 14	9.8 ± 0.4	6.6	0.48
902	340.84	−0.30	110 ± 30	12.5 ± 0.4	5.4	0.73
933	305.49	0.11	29 ± 12	6.8 ± 0.9	7.1	0.63
964	345.57	0.79	3 ± 2	1.9 ± 0.6	6.4	0.75
Taurus	171.6	−15.8	0.11	0.141 ± 0.007	8.4	5.6
Lupus	338.9	16.5	0.04	0.189 ± 0.009	8.2	1.0
Orion A	209.1	−19.9	0.55	0.43 ± 0.02	8.4	3.0
Cepheus	110.7	12.6	2.13	0.92 ± 0.05	8.6	2.5
MonOB1	202.1	1.0	1.33	0.75 ± 0.03	9.1	2.4
Maddalena	216.5	−2.5	5.29	2.1 ± 0.1	10.1	1.2
Sgr B	0.65	−0.05	150	7.9 ± 0.8	0.1	2.3

Cloud	R_{gal} [kpc]	$\rho_{0,CR}$ [10^{-12} GeV^{-1} cm^{-3}]	α
418	10.6	1.7 ± 0.5	2.69 ± 0.05
429	10.3	1.4 ± 0.4	2.74 ± 0.05
Maddalena	10.1	1.8 ± 0.6	2.93 ± 0.06
MonOB1	9.1	1.9 ± 0.6	2.99 ± 0.06
610	8.9	2.3 ± 1.1	2.79 ± 0.04
612	8.7	1.3 ± 0.4	2.80 ± 0.09
Cepheus	8.6	1.7 ± 0.5	2.87 ± 0.07
OrionA	8.4	1.5 ± 0.5	2.83 ± 0.05
Taurus	8.4	1.4 ± 0.5	2.89 ± 0.05
Lupus	8.2	1.1 ± 0.4	2.74 ± 0.10
933	7.1	3.2 ± 1.1	2.69 ± 0.02
900	6.6	2.7 ± 0.8	2.74 ± 0.03
964	6.4	1.3 ± 0.4	2.56 ± 0.04
876	6.0	2.3 ± 0.7	2.82 ± 0.03
243	5.8	4.8 ± 1.4	2.86 ± 0.03
877	5.5	3.9 ± 1.2	2.69 ± 0.02
902	5.4	4.4 ± 1.3	2.74 ± 0.02
804	4.6	3.0 ± 0.9	2.61 ± 0.02
Sgr B	0.1	0.98 ± 0.06	2.80 ± 0.03
AMS02		1.12	2.8[a]

[a]From fitting of experimental points on the energy range 20–200 GeV.

Aharonian et al. 2020

Outline

- Galactic cosmic-ray (CR) spectrum: direct and indirect studies
- The interstellar medium and molecular clouds
- Previous CR estimations through the MCs study with Fermi-LAT
- Selected MCs, analysis technique with Fermi-LAT and the results
- Theoretical interpretation
- Summary and future perspectives

Selected molecular clouds

Name	l	b	D	A	Angular area
	(deg)	(deg)	(pc)	($10^5 M_\odot/kpc^2$)	deg^2
Aquila Rift	24.14	12.48	225	16.02	104
Taurus	171.04	-15.32	135	5.63	32
Rho Oph	354.34	16.82	125	3.98	24
Orion A	211.83	-18.80	490	3.83	26
Cepheus	107.94	15.07	860	3.73	29
Orion B	205.14	-13.69	490	2.89	14

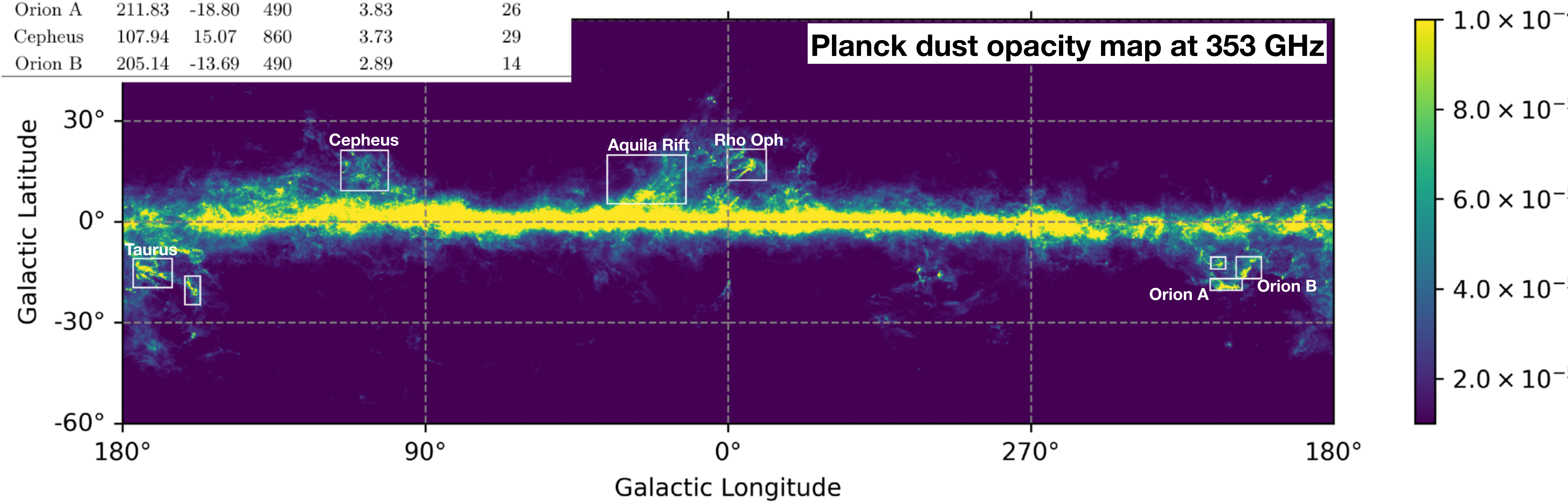

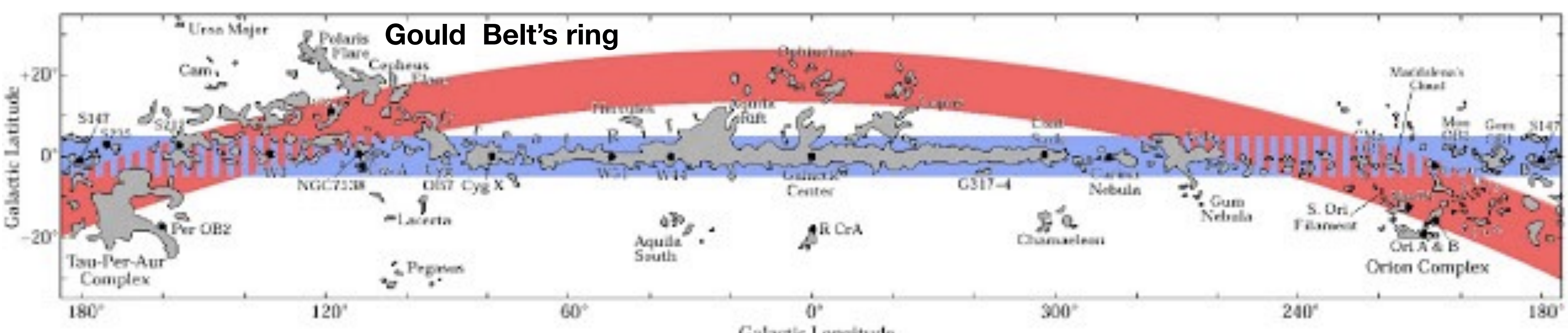

Short about the analysis

Data selection

- Time period: 2008 Aug 04-2019 Aug 04
- Energy range: 3 GeV - 1 TeV

Standard analysis of selected 4 regions using Fermipy

- 4 spatial templates have been considered during each analysis: Cloud and diffuse galactic based on Planck dust maps, IC galprop and standard Fermi extragalactic isotropic emission templates
- 4FGL catalog
- PL model for cloud and Galactic diffuse emission

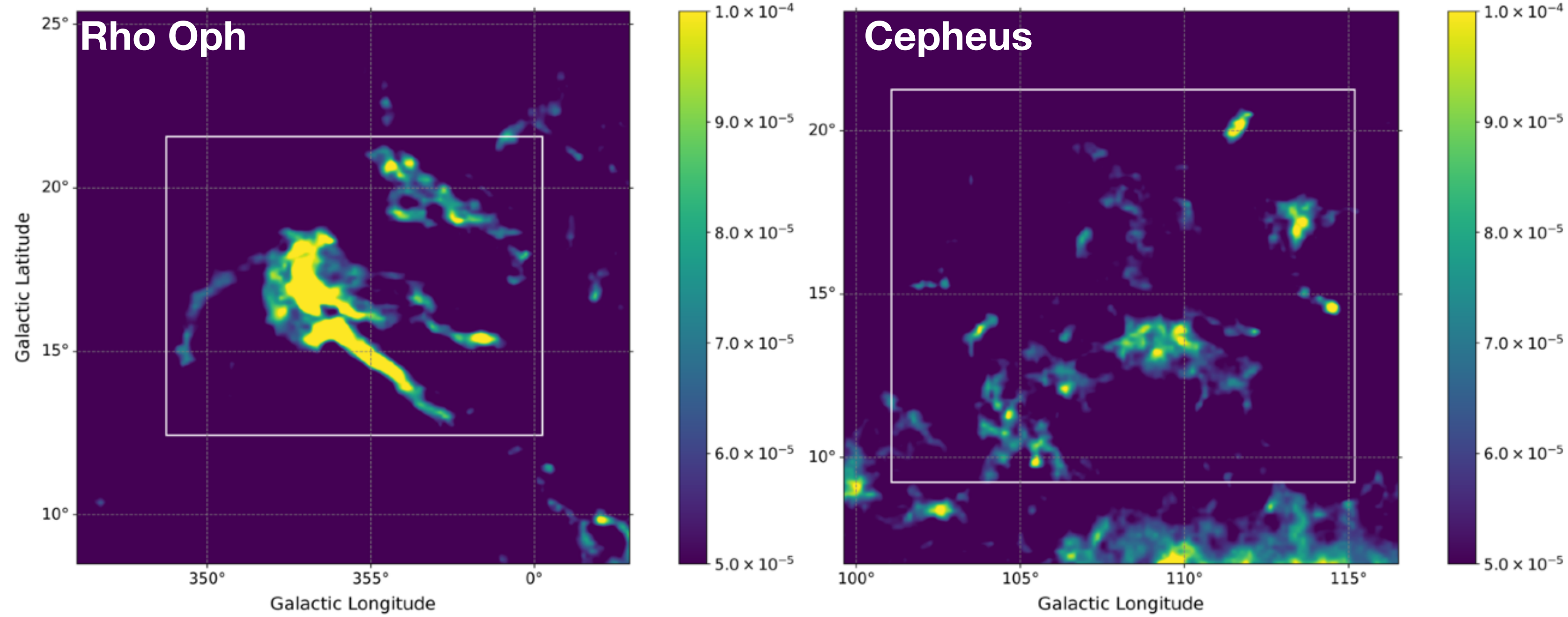

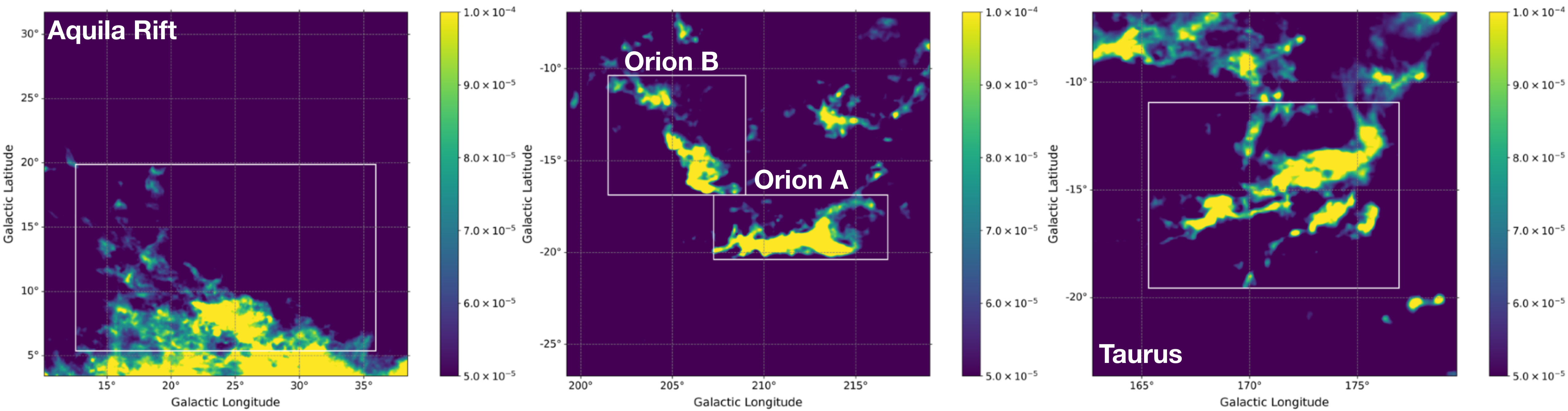

Planck dust opacity map at 353 GHz

HE gamma-ray production inside the cloud via pion decay

Inelastic collisions of CR protons with the ambient matter in the molecular cloud

$$p_{CR} + p_{MC} \rightarrow p + p + \pi^0$$

Then pions decay very quickly into two protons via the dominant decay mode.

$$\pi^0 \rightarrow \gamma + \gamma$$

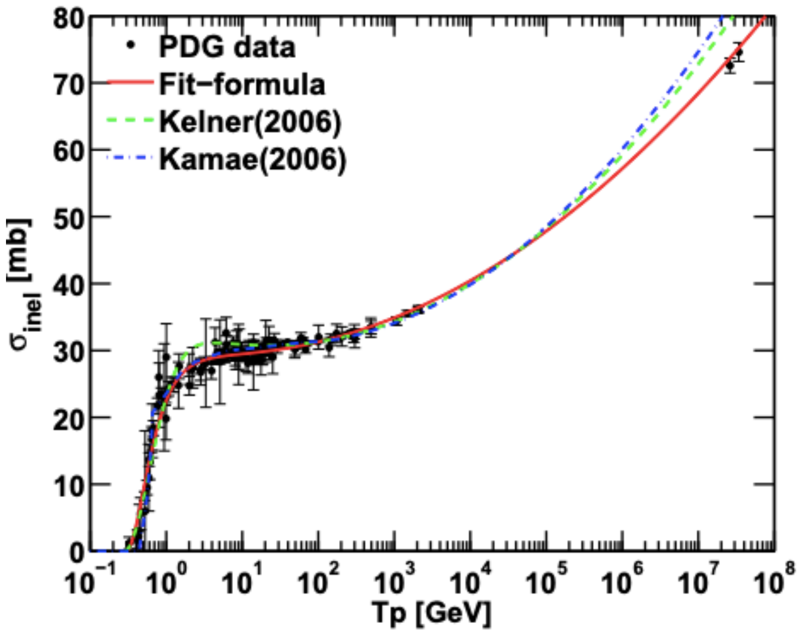

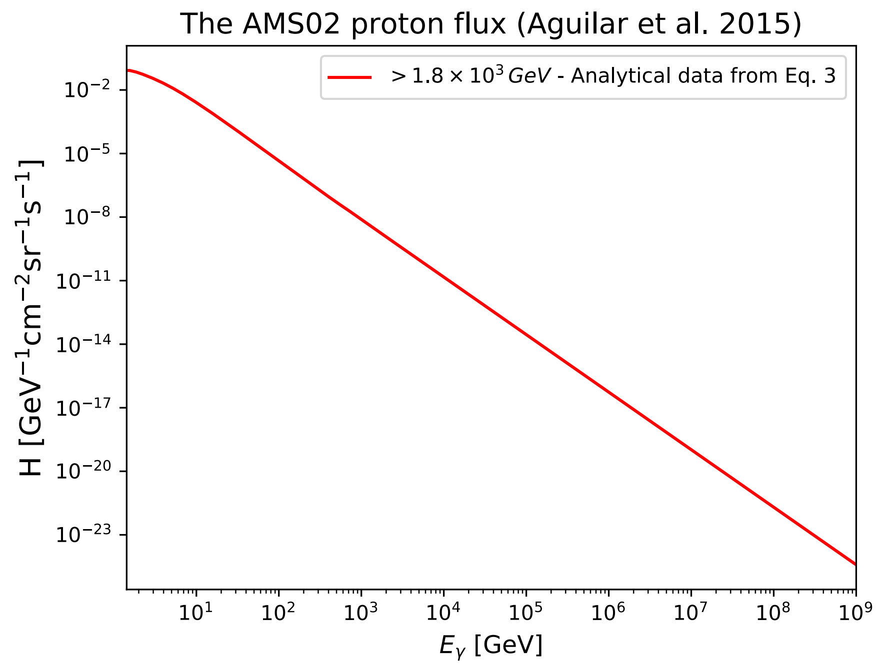

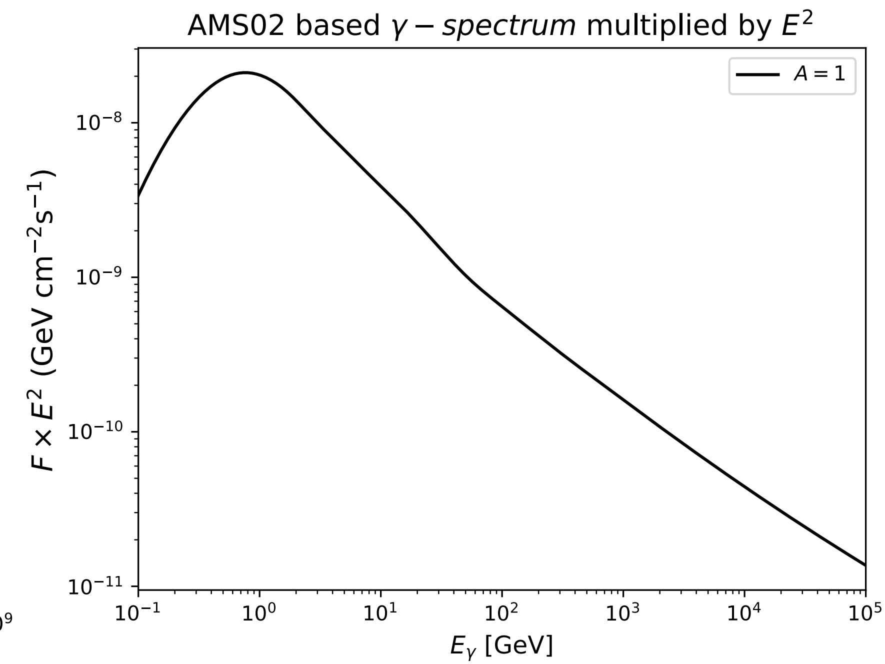

The total p–p inelastic cross section (Kafexhiu et al. 2014)

$$F_\gamma(E_\gamma) = 1.25 \times 10^{19} A \xi_N \int dE_p \frac{d\sigma}{dE_\gamma} F_p(E_p) \; (A = M_5/d_{kpc}^2, M_5 = M/M_{Sun})$$

CR proton spectrum reported by the AMS-02 (Aguilar et al. 2015)

$$M = m_H N_H A_{cloud} = m_H \tau_D / \left(\frac{\tau_D}{N_H}\right)^{ref} A_{angular} D^2 \qquad \left(\frac{\tau_D}{N_H}\right)^{ref} = (1.18 \pm 0.17) \times 10^{-26} cm^2$$

$\xi_N = 1.8$ enhancement factor includes contribution of heavy nuclei from both the interstellar medium and CRs

Derived gamma-ray spectra

Table 2. The best fit power-law parameters of γ-ray spectral analysis in comparison with AMS-02-based γ-ray spectrum in the 3 GeV–1 TeV energy range.

Name	TS	Photon index (Γ)	Flux at 3 GeV ($10^{-10} \times$ erg cm^{-2} s^{-1})	AMS-02-based Flux at 3 GeV ($10^{-10} \times$ erg cm^{-2} s^{-1})
Aquila Rift	21547	2.64 ± 0.01	6.27 ± 0.09	3.11 ± 0.46
Taurus	8319	2.72 ± 0.03	1.34 ± 0.04	1.09 ± 0.16
Rho Oph	6381	2.67 ± 0.03	1.56 ± 0.05	0.77 ± 0.11
Orion A	9583	2.78 ± 0.03	1.07 ± 0.03	0.74 ± 0.11
Cepheus	6899	2.77 ± 0.03	1.24 ± 0.03	0.72 ± 0.11
Orion B	4899	2.84 ± 0.04	0.74 ± 0.03	0.56 ± 0.08

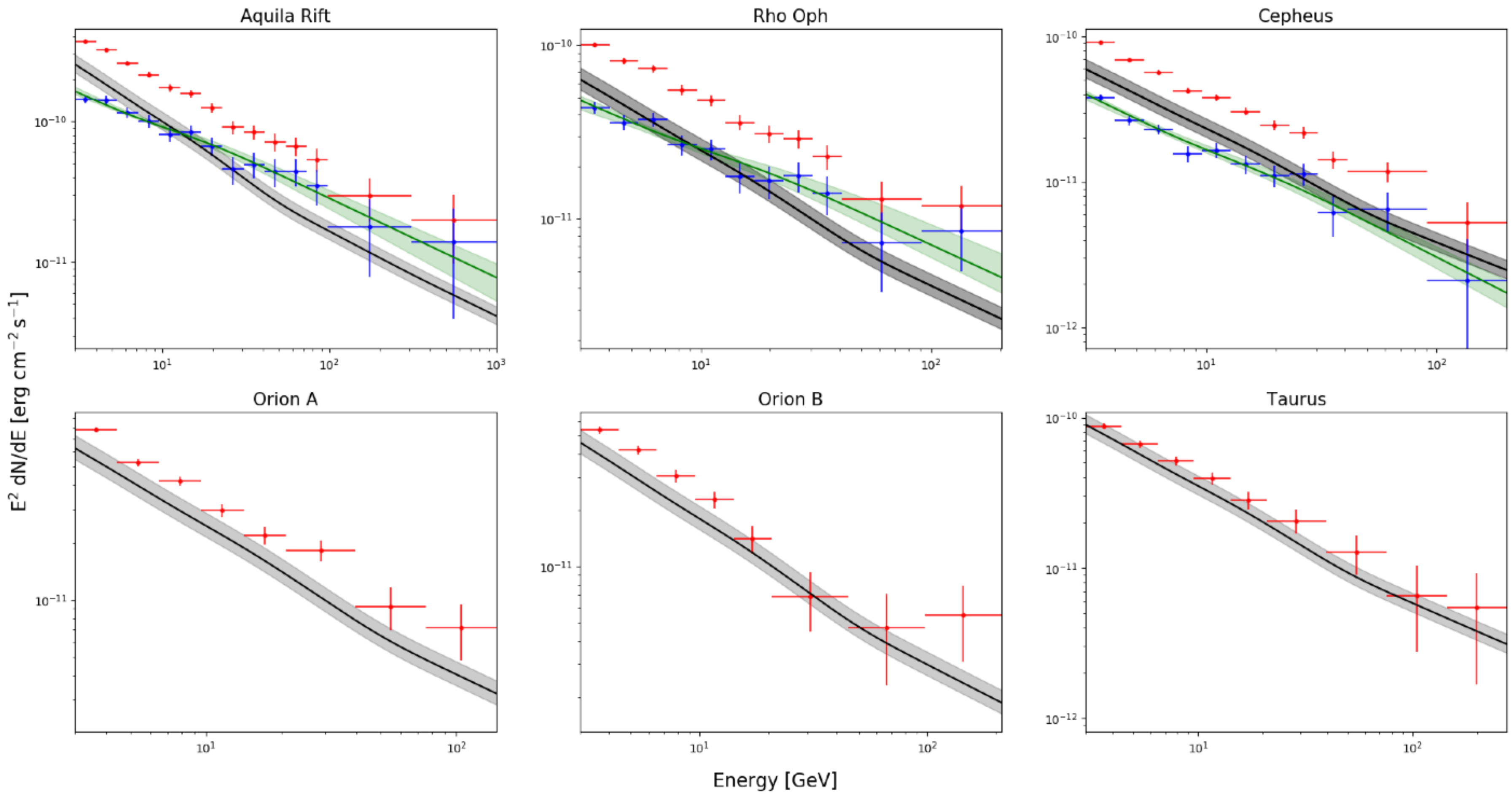

The enhanced CR spectra of three MCs obtained from fitting the excess γ-ray spectrum

Table 3. The enhanced CR power-law spectral indexes and CR densities calculated at 10 GeV.

Name	$\rho_{0,\mathrm{CR}}$	α
	$10^{-12} \times \mathrm{GeV}^{-1}\mathrm{cm}^{-3}$	
Aquila Rift	0.69 ± 0.28	2.62 ± 0.05
Rho Oph	0.86 ± 0.43	2.67 ± 0.08
Cepheus	0.91 ± 0.41	2.86 ± 0.08
AMS-02	1.05	2.80

$$dN_p/dE = F_0(E/E_0)^{-\alpha}$$

$$\rho_{0,CR} = \frac{F_0}{V} = \frac{m_p}{10^5 M_\odot} \frac{< n_H >}{d_{kpc}^2} A F_0 \ (A = M_5/d_{kpc}^2)$$

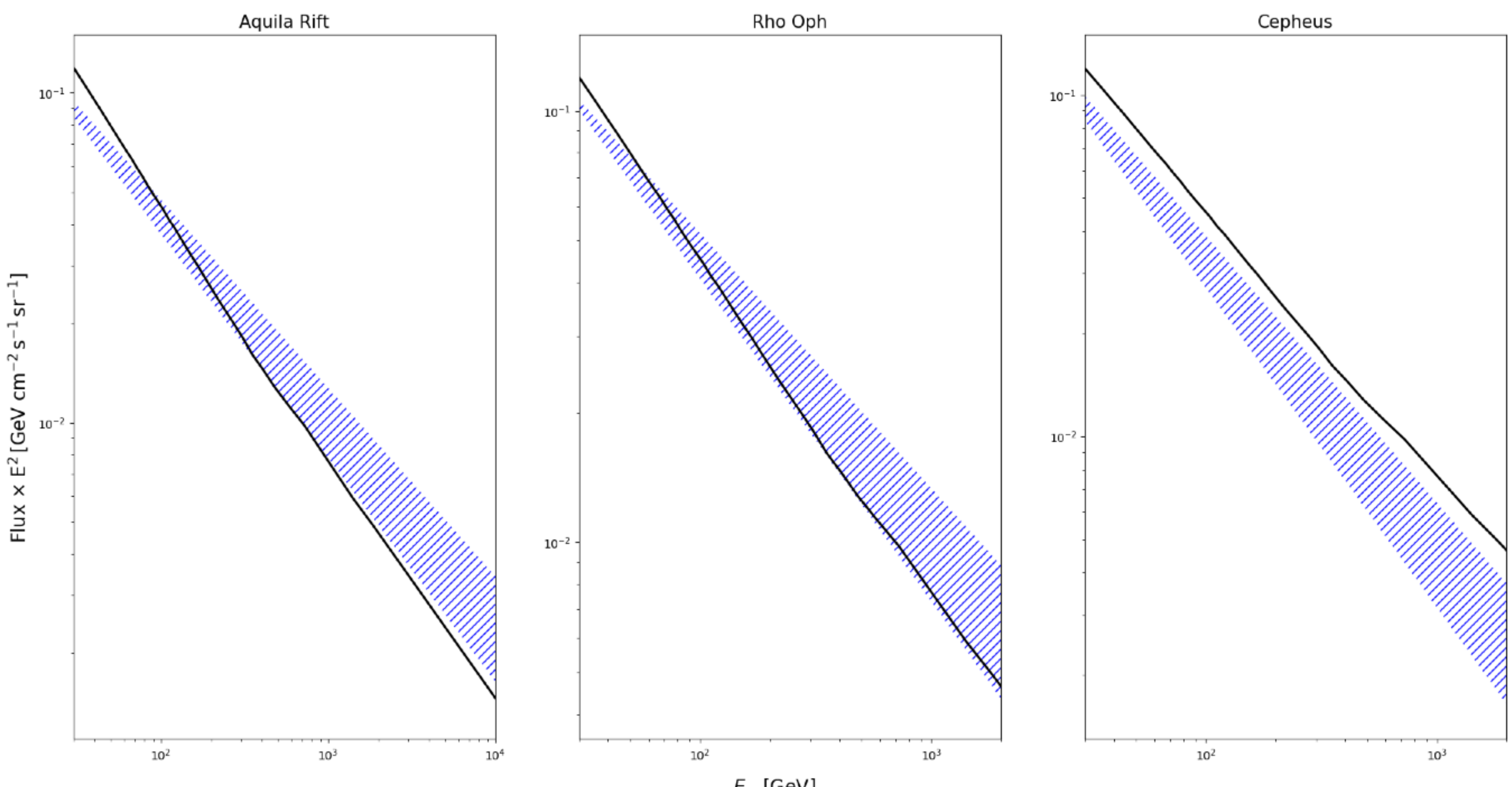

Outline

- Galactic cosmic-ray (CR) spectrum: direct and indirect studies
- The interstellar medium and molecular clouds
- Previous CR estimations through the MCs study with Fermi-LAT
- Selected MCs, analysis technique with Fermi-LAT and the results
- Theoretical interpretation
- Summary and future perspectives

Star formation: stellar winds

OB associations consist largely of very young, massive stars (about 10 to 50 solar masses) of spectral types O and B, which have an absolute L≈ 10^5 L_sun luminosity.

R associations consist of young, bright stars of intermediate mass (3 to 10 solar masses).

T associations contain mostly T Tauri stars. These are comparatively cool, newly formed stars of low mass (3 or less solar masses) that are still in the process of contraction. They are characterized by irregular variations of light and low luminosity.

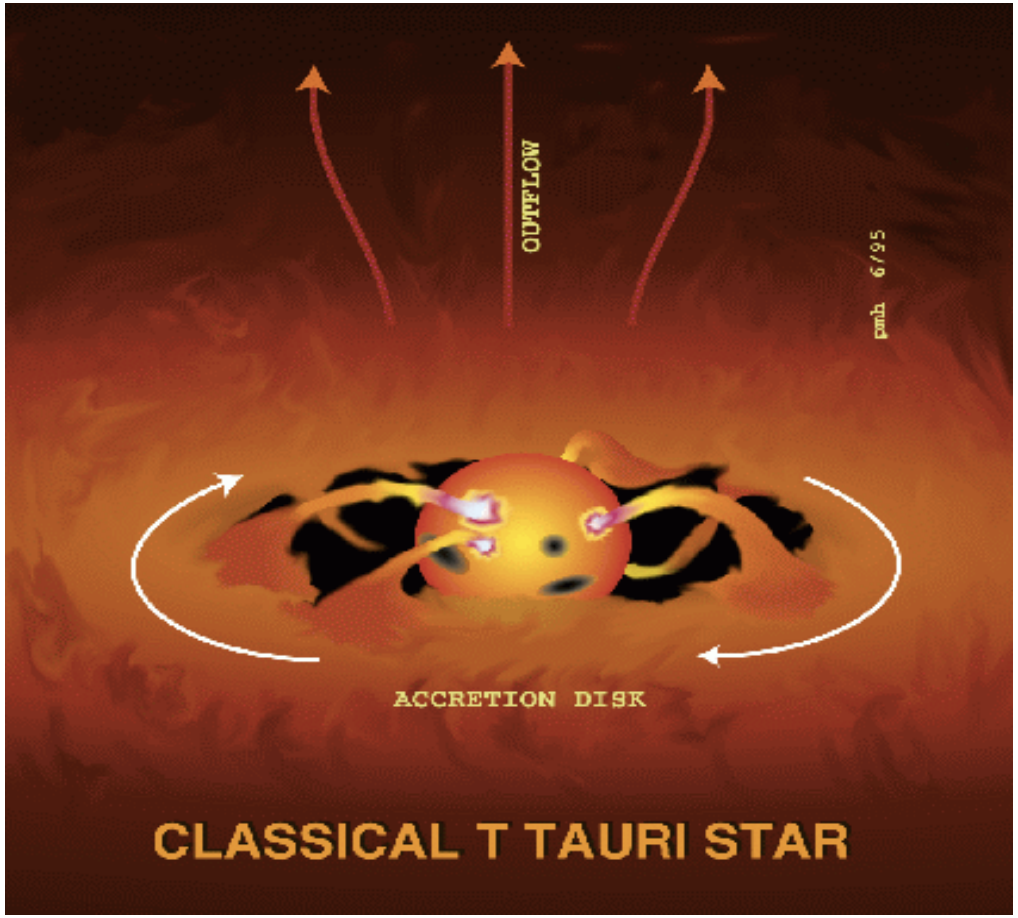

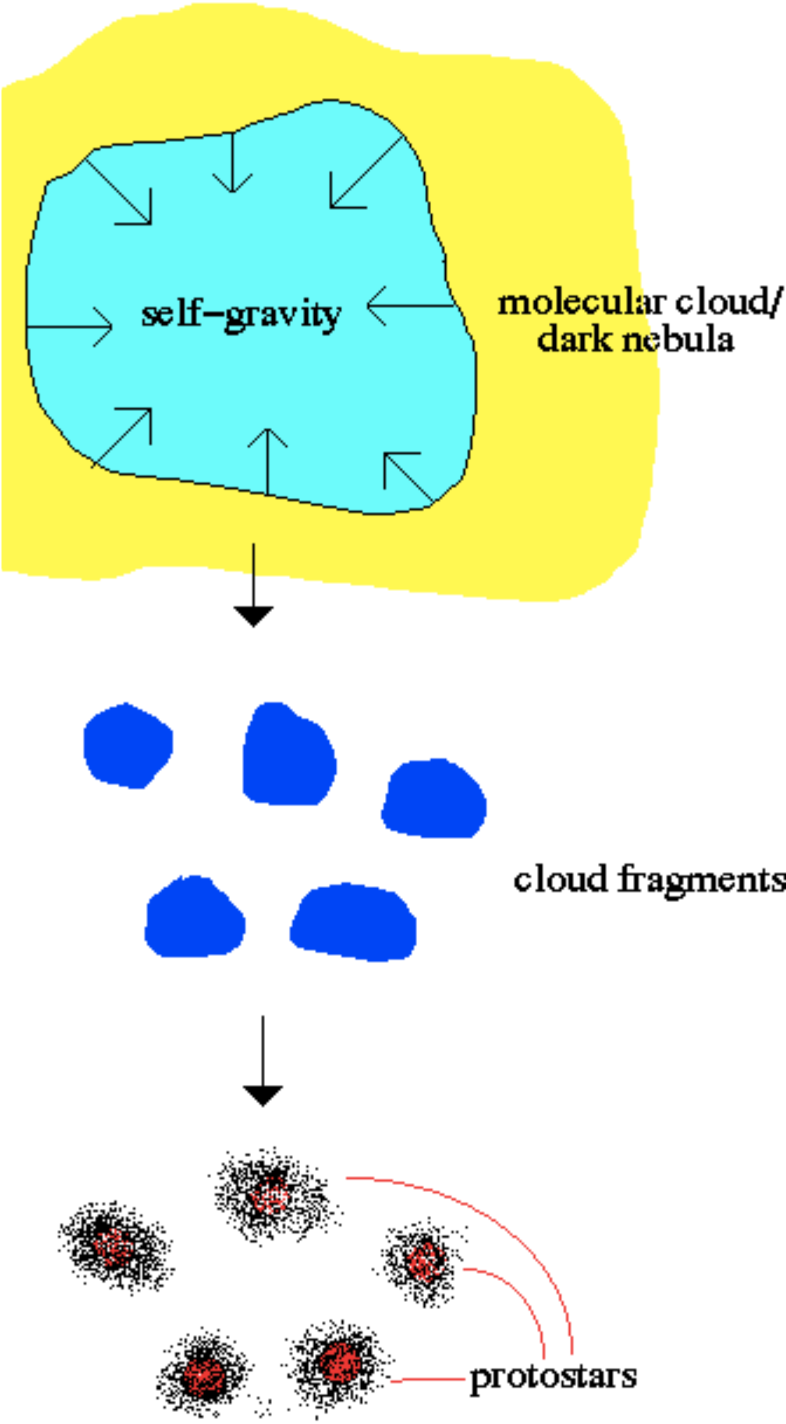

Stellar winds as alternative CR accelerators

Stellar populations

- **Cepheus:** Contains several star-forming regions such as three nearby OB associations (Kun et al. 2008).
- **Rho Oph:** Several hundred T-Tauri stars (Bontemps et al. 2001).
- **Aquila Rift:** No star-forming regions in the analysed region of this cloud.

Contribution of stellar winds and supernovae to cosmic rays and gamma rays in the Galaxy

Scale	Medium (distance)	Stellar winds important for:	Supernovae important for:	Remarks
Very small ($\lesssim$1 pc)	Dark clouds ($\lesssim$200 pc)	T associations, if CR confinement strong enough: γ-ray sources?	if chance collision with field SNRs: γ-ray sources	ρOph cloud only known possible example
Small ($\sim$10–100 pc)	Molecular clouds ($\lesssim$3 kpc)	OB associations, if WR present (Carina, Cygnus): γ-ray sources $\bar{p}$ in CR very high-energy CR?	OB associations, if SN present (SNOBs): γ-ray sources $\bar{p}$ in CR	Average OB associations ('Orion-like') invisible as γ-ray sources
Medium ($\lesssim$1–2 kpc)	Solar neighborhood ($\lesssim$2.5 kpc) Gould Belt ($\lesssim$500 pc)	^{22}Ne excess in CR from isolated WC; diffuse γ-ray features	Local CR; diffuse γ-ray features	$\bar{P}_s/\bar{P}_w$ = 5 or 20 (depending on SN progenitors)
Large	Galaxy	dominant contribution to GCR from WR in the inner galaxy? part of diffuse γ-ray emission	probable major contribution to GCR; part of diffuse γ-ray emission	gives SN acceleration efficiency: η_s = 2.5 to 10%

Cesarsky & Montmerle 1983

Table 3. The enhanced CR power-law spectral indexes and CR densities calculated at 10 GeV.

Name	$\rho_{0,\mathrm{CR}}$ $10^{-12}\times\mathrm{GeV}^{-1}\mathrm{cm}^{-3}$	α
Aquila Rift	0.69 ± 0.28	2.62 ± 0.05
Rho Oph	0.86 ± 0.43	2.67 ± 0.08
Cepheus	0.91 ± 0.41	2.86 ± 0.08
AMS-02	1.05	2.80

Summary and future perspectives

- The comparison of γ-ray spectra of Taurus, Orion A, and Orion B clouds with the AMS-02 based model confirms them as passive clouds.
- A similar comparison of Aquila Rift, Rho Oph, and Cepheus spectra yields significant deviation in both spectral indices and absolute fluxes, which can imply an additional acceleration of CRs throughout the entire clouds.
- The excess CR spectrum gives a considerable amount of an enhanced CR energy density and it shows a significant deviation in spectral shapes compared to the average AMS-02 CR spectrum between 30 GeV and 10 TeV.
- We suggest that this variation in the CR spectrum of Cepheus and Rho Oph could be accounted for by an efficient acceleration in the shocks of winds of stars populated the whole cloud. The absolute excess CR in case of Aquila Rift flux could be related to an additional acceleration of CRs by supernova remnants or propagation effects in the cloud.

Four clouds from the list including Rho Oph are in the FOV of LHASSO.

Properties of the GMCs in the FOV of LHAASO. The estimated distance and position are obtained from Dame et al, 1987. The mass values listed in the second column are calculated from the CfA maps (see [61] for detail).

Region	M [$10^5\ M_\odot$]	D [pc]	l [°]	b [°]	M/d^2 [($10^5\ M_\odot$/kpc^2)]	size [arcdeg^2]
ρ Oph	0.12	165	356	+18	8.4	68
Orion B	0.78	500	205	−14	3.9	22
Orion A	1.2	500	213	−18	5.2	28
Mon R2	1.1	830	214	−12	1.7	19
Taurus	0.30	140	170	−16	15.0	101
Polaris flare	0.055	230	130	+26	0.96	40

Currently, involved in a project of study of MCs in the Galactic plan with HESS and Fermi.

Names	GLON	GLAT	A_co	Catalog
	deg	deg		
243	42.04	-0.36	0.2	Rice et al. 2016
252	45.62	0.11	0.16	Rice et al. 2016
804	328.58	0.4	0.29	Rice et al. 2016
876	323.61	0.22	0.2	Rice et al. 2016
877	333.46	-0.31	0.25	Rice et al. 2016
902	340.84	-0.3	0.3	Rice et al. 2016
926	326.6	0.29	0.28	Rice et al. 2016
933	305.49	0.11	0.15	Rice et al. 2016
934	328.41	0.63	0.26	Rice et al. 2016
964	345.57	0.79	0.2	Rice et al. 2016
57	2.21	-0.21	0.0	Miville-Deschenes et al.
78	2.93	0.27	0.0	Miville-Deschenes et al.
148	342.2	0.26	0.0	Miville-Deschenes et al.
1155	3.93	-1.02	0.0	Miville-Deschenes et al.
1312	351.5	0.22	0.0	Miville-Deschenes et al.

Thank You for Your Attention